Journal of Alloys and Compounds 509 (2011) 8840–8844

Contents lists available at ScienceDirect

Journal of Alloys and Compounds

journal homepage: www.elsevier.com/locate/jallcom

Microwave dielectric properties of temperature stable $Li_2Zn_xCo_{1-x}Ti_3O_8$ ceramics

Liang Fang[a], Dongjin Chu[a,b], Huanfu Zhou[a,*], Xiuli Chen[a], Hui zhang[a], Baocheng Chang[b], Chunchun Li[a], Yuandong Qin[b], Xi Huang[a]

[a] State Key Laboratory Breeding Base of Nonferrous Metals and Specific Materials Processing, Key Laboratory of Nonferrous Materials and New Processing Technology, Ministry of Education, Guilin University of Technology, Jiangan Road 12#, Guilin, Guangxi 541004, China
[b] Guangxi New Future Information Industry Co., Ltd., Beihai 536000, China

ARTICLE INFO

Article history:
Received 11 November 2010
Received in revised form 20 June 2011
Accepted 21 June 2011
Available online 28 June 2011

Keywords:
Dielectric ceramic
Microstructure
Microwave
X-ray diffraction

ABSTRACT

The $Li_2Zn_xCo_{1-x}Ti_3O_8$ ($x = 0.2–0.8$) solid solution system has been synthesized by the conventional solid-state ceramic route and the effect of Zn substitution for Co on microwave dielectric properties of $Li_2CoTi_3O_8$ ceramics has also been investigated. The microwave dielectric properties of these ceramics show a linear variation between the end members for all compositions. The optimized sintering temperatures of $Li_2Zn_xCo_{1-x}Ti_3O_8$ ceramics increase with increasing content of Zn. The specimen with $x = 0.4$ sintered at 1050 °C/2 h exhibits an excellent combination of microwave dielectric properties with $\varepsilon_r = 27.7$, $Q_u \times f = 57{,}100$ GHz and $\tau_f = -1.0$ ppm/°C.

1. Introduction

To meet the requirement of miniaturization, low temperature co-fired ceramic (LTCC) is widely used in the fabrication of various modules such as band-pass filters, local oscillators and other devices [1–5]. In order to use cheaper and highly conductive internal electrode metals such as Ag (the melting point 961 °C) and Cu (the melting point 1050 °C) the potential dielectric ceramics for LTCC are required to have low sintering temperature as well as the appropriate dielectric constant (ε_r), high quality factor ($Q \times f$), and a near-zero temperature coefficient (τ_f). However, the sintering temperatures of most commercial microwave dielectric ceramics are usually above 1300 °C. One favored approach has involved investigations of the effect of eutectic or glass-forming additives on the properties of established microwave materials; however, in many cases, the additions produce a significant deterioration in $Q \times f$ values. Another approach involves studies of new systems with lower melting points.

Many studies have been focused on some Li-containing compounds with low sintering temperature and good microwave dielectric properties, such as $Li_{1+x-y}Nb_{1-3x-3y}Ti_{x+4y}O_3$ ($x = 0.1$, $y = 0.05–0.175$) ceramics [6–8], Li_3NbO_4 [9], $Ca(Li_{1/3}Nb_{2/3})O_3$ [10,11], $Li_{0.5}Sm_{0.5}WO_4$ [12], $Ba_4LiNb_{3-x}Ta_xO_{12}$ ($x = 0–3$) [13] and Li_2MgSiO_4 [14]. More recently, the microwave dielectric properties of cubic spinels $Li_2ATi_3O_8$ (A = Zn, Mg, Co) [15–18] and $Li_2Mg_{1-x}Zn_xTi_3O_8$ [19] have been reported. These ceramics could be readily sintered to high density below 1100 °C and are characterized by high permittivities up to 28.9 and quality factors up to 72,000 GHz. The crystal structures of lithium spinels $Li_2MTi_3O_8$ (M = Zn, Mg, Co) have been reported by West et al. [20], where M cations show a strong preference for tetrahedral coordination and 1:3 cation ordering of Li/M and Ti occurs on the octahedral sites.

Considering that $Li_2ZnTi_3O_8$ has a negative τ_f of −11.2 ppm/°C and $Li_2CoTi_3O_8$ has a positive τ_f of 7.4 ppm/°C, further studies of $Li_2Zn_xCo_{1-x}Ti_3O_8$ solid solutions may reveal potential materials with τ_f close to zero. In addition, Shannon's effective ionic radius and polarizability of Co^{2+} are very similar to those of Zn^{2+} [21,22], and the substitution of Zn for Co to form $Nd(Co_{1-x}Zn_x)_{1/2}Ti_{1/2}O_3$ ($x = 0.2$) [23] and $(Zn_xCo_{1-x})Ta_2O_6$ ($x = 0.05$) [24] solid solutions have been reported to effectively improve the dielectric properties of the ceramics. Likewise, it is worthwhile to investigate whether intermediate $Li_2Zn_xCo_{1-x}Ti_3O_8$ ($0 < x < 1$) ceramics might exhibit equivalent or superior properties compared to those end members. In this paper, the synthesis, structure, and dielectric properties of $Li_2Zn_xCo_{1-x}Ti_3O_8$ ($x = 0.2–0.8$) solid solutions were investigated and the effects of Zn substitution for Co on microwave dielectric properties of $Li_2CoTi_3O_8$ ceramics were also reported.

2. Experimental procedures

Specimens of the $Li_2Zn_xCo_{1-x}Ti_3O_8$ ceramics were prepared by a conventional mixed oxide route from the high-purity oxide powders of Li_2CO_3 (≥99.9%), Co_2O_3 (≥99%), ZnO (≥99.5%) and TiO_2 (≥99.9%). Stoichiometric amounts of the powders

* Corresponding author.
E-mail address: zhouhuanfu@163.com (H. Zhou).

0925-8388/$ – see front matter © 2011 Published by Elsevier B.V.
doi:10.1016/j.jallcom.2011.06.093

were weighed and milled in alcohol medium using zirconia balls for 4 h. The mixtures were dried and calcined at 900 °C for 4 h. The calcined powders were ground well and mixed with 5 wt.% of polyvinyl alcohol (PVA, the hydrolysis level is 99%, the degree of polymerization is 1750, and the average molecular weight is about 77,000 g/mol) solution as the binder. The powders were then uniaxially pressed into cylindrical disks of 12 mm diameter and 6–7 mm height under a pressure of 200 MPa. The samples were heated at 550 °C for 4 h to remove the organic binder and then sintered at 1000–1100 °C for 2 h.

The bulk densities of the sintered ceramics were measured by the Archimedes method. The phase compositions of calcined powders and sintered pellets were determined using an X-ray diffractometer (XRD) (CuK_α, 1.54059 Å, Model X'Pert PRO, PANalytical, Almelo, Holland). The sintered samples were polished and thermally etched at temperatures 50 °C lower than their respective sintering temperatures for 30 min. The surface micrographs of the samples were examined using a scanning electron microscope (SEM, Model JSM6380-LV, JEOL, Tokyo, Japan). The microwave dielectric properties were measured using a network analyzer (Model N5230A, Agilent Co., Palo Alto, CA) and a temperature chamber (Delta 9039, Delta Design, San Diego, CA). The relative permittivity was calculated using TE_{011} mode under the end-shorted condition using the method suggested by Hakki and Coleman, modified by Courtney [25,26]. The temperature coefficients of resonant frequency τ_f were calculated by the formula as follows:

$$\tau_f = \frac{f_T - f_0}{f_0(T - T_0)} \quad (1)$$

where f_T, f_0 are the resonant frequencies at the measuring temperatures T (85 °C) and T_0 (25 °C), respectively.

3. Results and discussion

The room temperature XRD patterns recorded for the $Li_2Zn_xCo_{1-x}Ti_3O_8$ (x = 0.2–0.8) ceramics sintered at 1050 °C using Cu Kα radiation are shown in Fig. 1. The patterns are similar and match well with PDF files No. 00-049-0449 of $Li_2CoTi_3O_8$. All of the peaks were indexed and there was no evidence of any secondary phases present. The system $Li_2Zn_xCo_{1-x}Ti_3O_8$ crystallizes in a cubic spinel structure with space group $P4_332$, and the solid solutions of $Li_2Zn_xCo_{1-x}Ti_3O_8$ are easily formed for all x values since the Shannon's effective ionic radii are similar (0.745 Å to Co^{2+} radii and 0.74 Å to Zn^{2+} radii) and Zn^{2+} and Co^{2+} are isovalent [21].

Fig. 2 presents the relative densities of the $Li_2Zn_xCo_{1-x}Ti_3O_8$ (x = 0.2–0.8) ceramics as a function of sintering temperature from 1000 °C to 1100 °C. As the sintering temperature increases, the relative density of the specimen gradually increases to an optimized value and thereafter slightly decreases, which might be attributed to trapped porosity caused by the volatilization of lithium and zinc and abnormal grain growth [19]. In addition, the optimized sintering temperature increases gradually from 1025 °C to 1075 °C as the amount of Zn substitution increases since the optimum sintering temperature of pure $Li_2ZnTi_3O_8$ (~1075 °C) is a little higher than that of $Li_2CoTi_3O_8$ (~1025 °C).

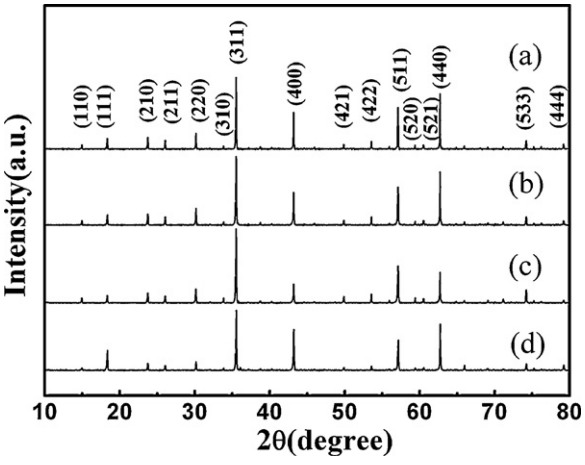

Fig. 1. XRD patterns of $Li_2Zn_xCo_{1-x}Ti_3O_8$ (x = 0.2–0.8) ceramics: (a) x = 0.2; (b) x = 0.4; (c) x = 0.6; (d) x = 0.8.

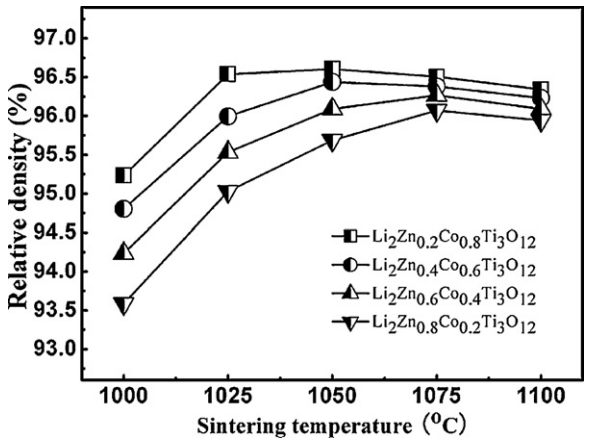

Fig. 2. The relative densities of the $Li_2Zn_xCo_{1-x}Ti_3O_8$ (x = 0.2–0.8) ceramics as a function of sintering temperature from 1000 °C to 1100 °C for 2 h.

The thermally etched surface microstructures of $Li_2Zn_xCo_{1-x}Ti_3O_8$ ceramics sintered at different temperatures for 2 h are illustrated in Fig. 3. The well-sintered and uniform microstructures of $Li_2Zn_xCo_{1-x}Ti_3O_8$ solid solution could be achieved at optimized sintering temperature from 1025 °C to 1075 °C, as shown in Fig. 3(a–f). It is notable that the grain size of $Li_2Zn_xCo_{1-x}Ti_3O_8$ ceramics increases with increasing sintering temperatures whereas decreases with the amount of Zn substitution. For the $Li_2Zn_{0.4}Co_{0.6}Ti_3O_8$ sintered at 1000 °C, the microstructure is observed with several pores, and most of the grain sizes are small, approximately 4 (m, as shown in Fig. 3(g). As the sintering temperature increases from 1000 °C to 1050 °C, the ceramic exhibits a dense microstructure. However, as the sintering temperature exceeds 1075 °C, abnormal grain growth occurs. A few large grains with an average size of 50 (m and a small amount of trapped porosity probably caused by the volatilization of lithium [1,17] and zinc are observed, as shown in Fig. 3(j).

Fig. 4 shows the variation of permittivity as a function of sintering temperature for $Li_2Zn_xCo_{1-x}Ti_3O_8$ (x = 0.2–0.8) ceramics. The permittivity is affected significantly by sintering temperature and compositions. For the $Li_2Zn_xCo_{1-x}Ti_3O_8$ (x = 0.2–0.8) ceramics, the permittivities firstly increase with increasing the sintering temperature to the optimized sintering temperature due to the increase of relative density, and then slightly decrease, which might be attributed to the deficiencies of Li and Zn, which leads to the decrease in density and lattice defects [19,27]. In addition, as x increases from 0.2 to 0.8, the permittivities of $Li_2Zn_xCo_{1-x}Ti_3O_8$ (x = 0.2–0.8) samples sintered at optimized temperature decrease from 28.11 to 26.94, which is mostly due to lower relative density with increasing Zn content, though the average ionic polarizability (α_D^T/V_m, where α_D^T is the sum of ionic polarizability of individual ions, and V_m is the molar volume) calculated from modified Clausius–Mossotti equation increases slightly as the amount of Zn substitution increases.

Fig. 5 shows the variation of unloaded quality factor ($Q_u \times f$) as a function of sintering temperature for $Li_2Zn_xCo_{1-x}Ti_3O_8$ (x = 0.2–0.8) ceramics. It is expected that the $Q_u \times f$ values of $Li_2Zn_xCo_{1-x}Ti_3O_8$ ceramics system vary linearly between end members $Li_2ZnTi_3O_8$ and $Li_2CoTi_3O_8$. Due to the increasing densities, the $Q_u \times f$ values first increase with the increasing sintering temperature and exhibit a maximum value of 53,500, 57,100, 60,900 and 65,800 GHz for the $Li_2Zn_xCo_{1-x}Ti_3O_8$ specimens (x = 0.2, 0.4, 0.6 and 0.8) sintered at the optimized temperature, respectively. Thereafter, the $Q_u \times f$ values slightly decrease with further increasing temperatures, which may be due to extrinsic factors, such as pore size, pore volume and the grain abnormal growth [27–29].

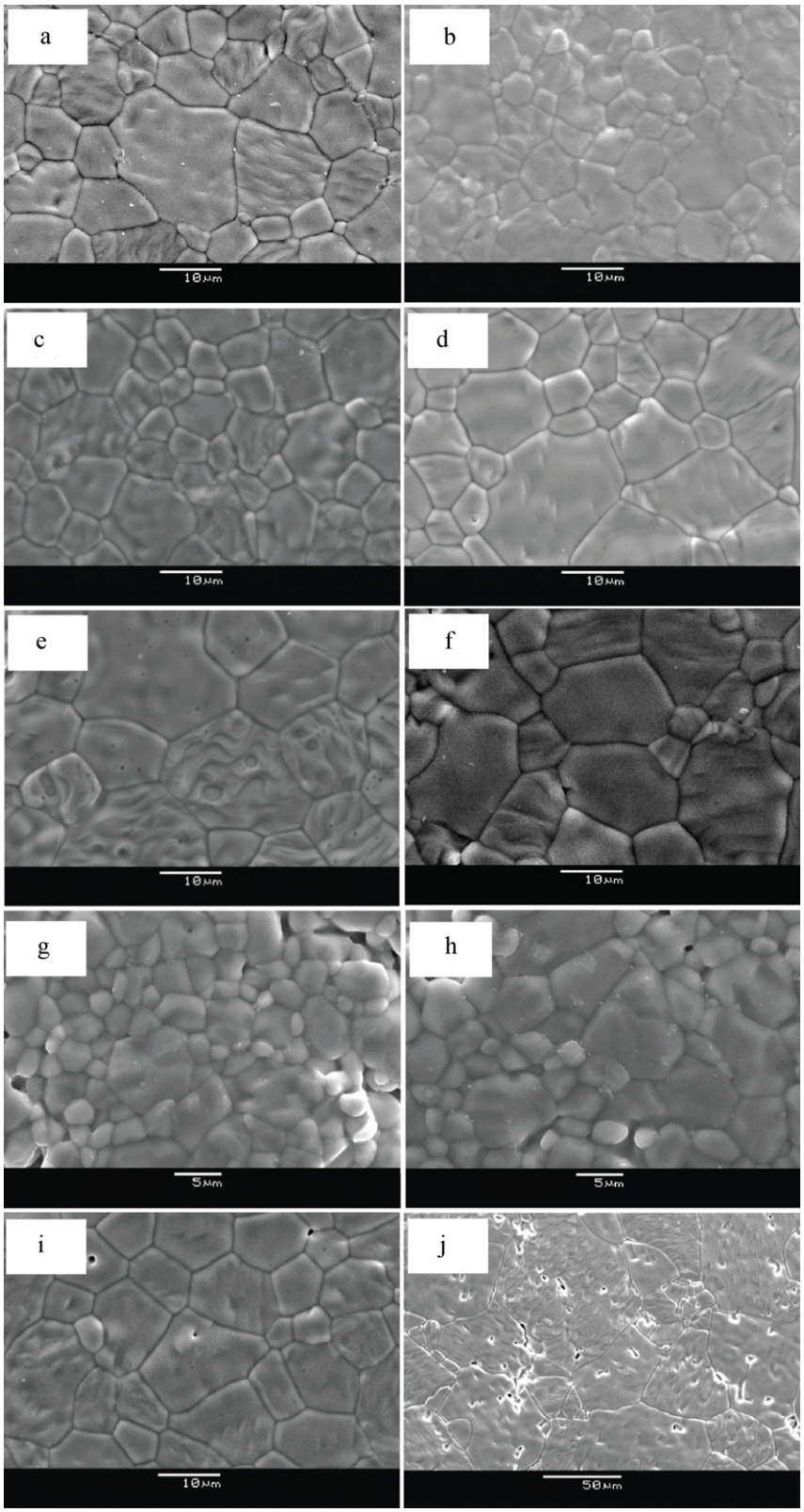

Fig. 3. The thermally etched surface microstructure of $Li_2Zn_xCo_{1-x}Ti_3O_8$ ceramics sintered at different temperatures for 2 h: (a) $x = 0$, at 1025 °C; (b) $x = 0.2$, at 1025 °C; (c) $x = 0.4$, at 1050 °C; (d) $x = 0.6$, at 1075 °C; (e) $x = 0.8$, at 1075 °C; (f) $x = 1$, at 1075 °C; (g) $x = 0.4$, at 1000 °C; (h) $x = 0.4$, at 1025 °C; (i) $x = 0.4$, at 1075 °C; (j) $x = 0.4$, at 1100 °C.

The variation of temperature coefficient of resonant frequency (τ_f) as a function of sintering temperature for $Li_2Zn_xCo_{1-x}Ti_3O_8$ ($x = 0.2$–0.8) ceramics is shown in Fig. 6. It is well known that the τ_f is governed by the composition and almost independent of the sintering temperature. As x increases from 0.2 to 0.8, the τ_f of $Li_2Zn_xCo_{1-x}Ti_3O_8$ ceramics varies from 5.3 to −11.3 ppm/°C. A near-zero τ_f of −1.0 ppm/°C could be achieved for $Li_2Zn_{0.4}Co_{0.6}Ti_3O_8$ sintered at 1050 °C for 2 h.

The microwave dielectric properties of the $Li_2Zn_xCo_{1-x}Ti_3O_8$ ($x = 0$–1) solid solution system under optimum sintering condi-

Table 1
Relative densities and microwave dielectric properties of the $Li_2Zn_xCo_{1-x}Ti_3O_8$ ($x = 0$–1) solid solution system sintered at the optimized temperature.

x	Sintering temperature (°C)	Relative density (%)	ε_r	$Q \times f$ (GHz)	τ_f (ppm/°C)	Ref.
$x = 0$	1025	97	28.9	52,600	7.4	[13]
$x = 0.2$	1025	96.5	28.11	53,500	3.8	–
$x = 0.4$	1050	96.4	27.7	57,100	−1.0	–
$x = 0.6$	1075	96.3	27.3	60,500	−5.8	–
$x = 0.8$	1075	96.1	26.94	65,800	−9.6	–
$x = 1$	1075	95	25.6	72,000	−11.2	[10,11]

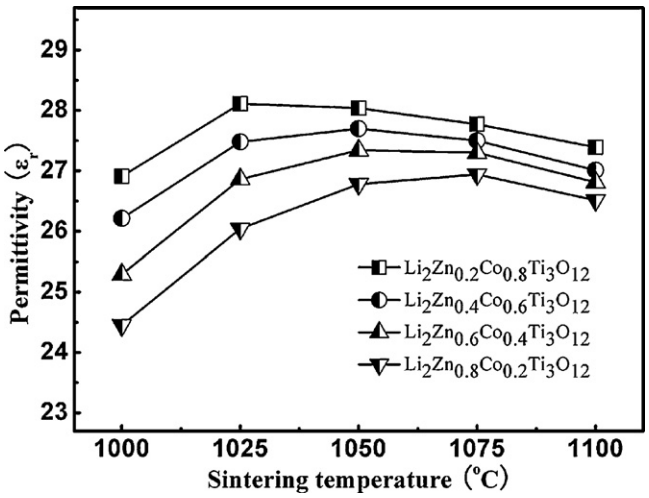

Fig. 4. The variation of permittivity as a function of sintering temperature for $Li_2Zn_xCo_{1-x}Ti_3O_8$ ($x = 0.2$–0.8) ceramics.

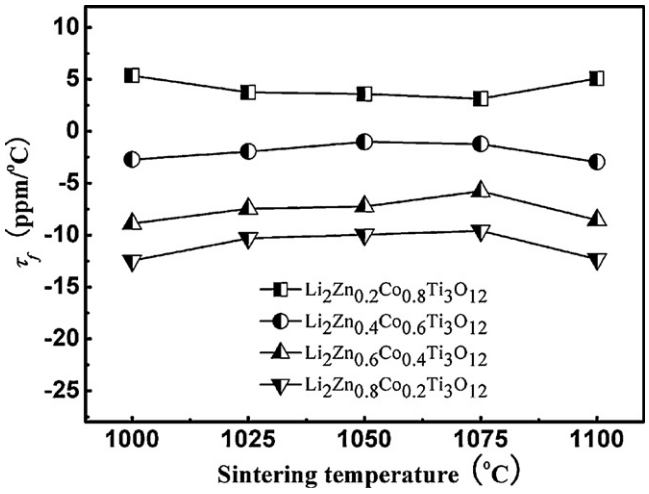

Fig. 6. The variation of temperature coefficient of resonant frequency (τ_f) as a function of sintering temperature for $Li_2Zn_xCo_{1-x}Ti_3O_8$ ($x = 0.2$–0.8) ceramics.

tions are summarized in Table 1, which are strongly related to the variation of composition. With the increasing content of Zn in the compositions, the permittivity slightly decreases from 28.9 to 25.6, the $Q_u \times f$ value increases from 52,600 to 72,000 and the τ_f gradually decreases from 7.4 to −11.2. It is noted that the specimen $Li_2Zn_{0.4}Co_{0.6}Ti_3O_8$ with $x = 0.4$ exhibits a near-zero τ_f of −1.0 ppm/°C in combination with a high $Q_u \times f$ of 57 100 GHz and a moderate ε_r of 27.7.

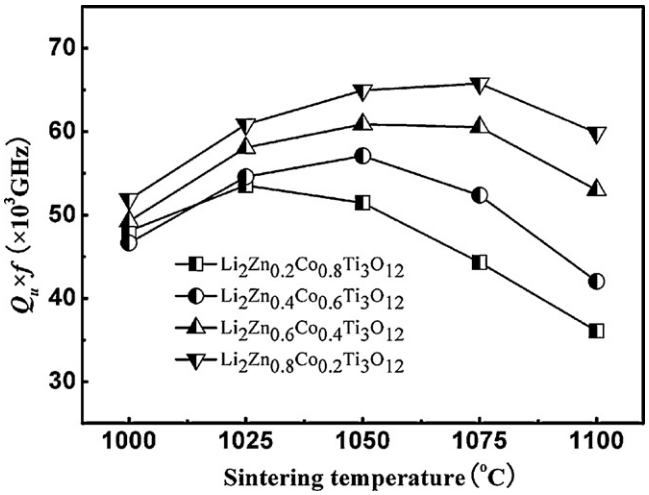

Fig. 5. The variation of quality factor ($Q_u \times f$) as a function of sintering temperature for $Li_2Zn_xCo_{1-x}Ti_3O_8$ ($x = 0.2$–0.8) ceramics.

4. Conclusions

The $Li_2Zn_xCo_{1-x}Ti_3O_8$ ($x = 0$–1) solid solution system with cubic spinel structure has been prepared by the conventional solid-state ceramic route. The microwave dielectric properties of these ceramics show a linear variation between those of the end members. The optimum sintering temperatures of $Li_2Zn_xCo_{1-x}Ti_3O_8$ ($x = 0.2$–0.8) ceramics increase from 1025 to 1075 °C with increasing x values. A moderate ε_r of 27.7, a high $Q_u \times f$ of 57,100 GHz and a near zero τ_f of −1.0 ppm/°C can be achieved for the $Li_2Zn_{0.4}Co_{0.6}Ti_3O_8$ ceramic sintered at 1050 °C/2 h. The main advantage of these materials is the low sintering temperature and further studies are in progress to reduce the sintering temperature below 950 °C to meet the requirement for LTCC applications.

Acknowledgments

This work was supported by Natural Science Foundation of China (Nos. 21061004 and 50962004), Natural Science Foundation of Guangxi (Nos. 0832003Z, 0832001 and 2011GXNSFB018012) and Programs for New Century Excellent Talents in Guangxi (No. 2006202).

References

[1] Z. Liang, L.L. Yuan, J.J. Bian, J. Alloys Compd. 509 (2011) 1893.
[2] Y.B. Chen, J. Alloys Compd. 509 (2011) 6884.
[3] C.L. Huang, Y.H. Chien, J. Alloys Compd. 509 (2011) L293.
[4] D. Chu, L. Fang, H. Zhou, X. Chen, Z. Yang, J. Alloys Compd. 509 (2011) 1931.
[5] M. Guo, S. Gong, G. Dou, D. Zhou, J. Alloys Compd. 509 (2011) 5988.
[6] A. Borosevich, P.K. Davies, J. Eur. Ceram. Soc. 21 (2000) 1719.
[7] A. Borisevich, P.K. Davies, J. Am. Ceram. Soc. 85 (2002) 2487.
[8] H.F. Zhou, H. Wang, D. Zhou, L.X. Pang, X. Yao, Mater. Chem. Phys. 109 (2008) 510.
[9] D. Zhou, H. Wang, L.X. Pang, X. Yao, X.G. Wu, J. Am. Ceram. Soc. 91 (2008) 4115.
[10] S. George, M.T. Sebastian, J. Alloys Compd. 473 (2009) 336.

[11] P. Liu, E.S. Kim, K.H. Yoon, Jpn. J. Appl. Phys. 40 (2001) 5769.
[12] H. Yang, Y. Lin, J. Zhu, F. Wang, Z. Dai, J. Alloys Compd. 502 (2010) L20.
[13] L. Fang, C.C. Li, X.Y. Peng, C.Z. Hu, B.L. Wu, H.F. Zhou, J. Am. Ceram. Soc. 93 (2010) 1229.
[14] S. George, P.S. Anjana, V.N. Deepu, P. Mohanan, M.T. Sebastian, J. Am. Ceram. Soc. 92 (2009) 1244.
[15] S. George, M.T. Sebastian, J. Am. Ceram. Soc. 93 (2010) 2164.
[16] F.H. Zhou, X.L. Chen, L. Fang, D.J. Chu, H. Wang, J. Mater. Res. 25 (2010) 1235.
[17] L. Fang, D.J. Chu, H.F. Zhou, X.L. Chen, Z. Yang, J. Alloys Compd. 509 (2011) 1880.
[18] X. Chen, H. Zhou, L. Fang, X. Liu, Y. Wang, J. Alloys Compd. 509 (2011) 5829.
[19] S. George, M.T. Sebastian, J. Eur. Ceram. Soc. 30 (2010) 2585.
[20] H. Kawai, M. Tabuchi, M. Nagata, H. Tukamoto, A.R. West, J. Mater. Chem. 8 (1998) 1273.
[21] R.D. Shannon, Acta Crystallogr. A 32 (1976) 751.
[22] R.D. Shannon, J. Appl. Phys. 73 (1993) 348.
[23] C.F. Tseng, J. Am. Ceram. Soc. 91 (2008) 4101.
[24] C.L. Huang, J.Y. Chen, J. Am. Ceram. Soc. 93 (2010) 470.
[25] B.W. Hakki, P.D. Coleman, IRE Trans. Microw. Theory Tech MTT-8 (1960) 402.
[26] W.E. Courtney, IEEE Trans. Microw. Theory Tech MTT-18 (1970) 476.
[27] D.J. Chu, L. Fang, H.F. Zhou, X.L. Chen, Z. Yang, J. Alloys Compd. 509 (2011) 1931.
[28] L. Fang, D.J. Chu, C.C. Li, H.F. Zhou, Z. Yang, J. Am. Ceram. Soc. 94 (2010) 524.
[29] J.D. Breeze, J.M. Perkins, D.W. McComb, N.M. Alford, J. Am. Ceram. Soc. 92 (2009) 671.